Environmental Science & Technology

ARTICLE

pubs.acs.org/est

Studying the Role of Common Membrane Surface Functionalities on Adsorption and Cleaning of Organic Foulants Using QCM-D

Alison E. Contreras,[†] Zvi Steiner,[‡] Jing Miao,[‡] Roni Kasher,[*,‡] and Qilin Li[*,†]

[†]Department of Civil and Environmental Engineering, Rice University, Houston Texas 77005, United States

[‡]Zuckerberg Institute for Water Research, The Jacob Blaustein Institutes for Desert Research, Ben-Gurion University of the Negev, Sde-Boqer campus 84990, Israel

Supporting Information

ABSTRACT: Adsorption of organic foulants on nanofiltration (NF) and reverse osmosis (RO) membrane surfaces strongly affects subsequent fouling behavior by modifying the membrane surface. In this study, impact on organic foulant adsorption of specific chemistries including those in commercial thin-film composite membranes was investigated using self-assembled monolayers with seven different ending chemical functionalities ($-CH_3$, $-O-$phenyl, $-NH_2$, ethylene-glycol, $-COOH$, $-CONH_2$, and $-OH$). Adsorption and cleaning of protein (bovine serum albumin) and polysaccharide (sodium alginate) model foulants in two solution conditions were measured using quartz crystal microbalance with dissipation monitoring, and were found to strongly depend on surface functionality. Alginate adsorption correlated with surface hydrophobicity as measured by water contact angle in air; however, adsorption of BSA on hydrophilic $-COOH$, $-NH_2$, and $-CONH_2$ surfaces was high and dominated by hydrogen bond formation and electrostatic attraction. Adsorption of both BSA and alginate was the fastest on $-COOH$, and adsorption on $-NH_2$ and $-CONH_2$ was difficult to remove by surfactant cleaning. BSA adsorption kinetics was shown to be markedly faster than that of alginate, suggesting its importance in the formation of the conditioning layer. Surface modification to render $-OH$ or ethylene-glycol functionalities are expected to reduce membrane fouling.

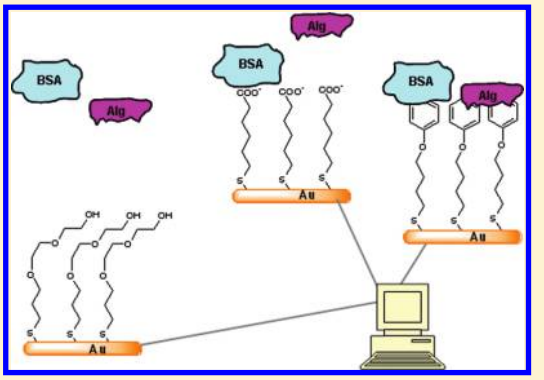

INTRODUCTION

Thin-film composite (TFC) membranes are widely used in reverse osmosis (RO) and nanofiltration (NF) systems for desalination, ultrapure water production, drinking water purification, and wastewater reuse.[1] A major hindrance to wider application of NF and RO for water treatment is fouling of the membrane by mineral precipitation (scaling), colloidal or dissolved organic matter,[2−4] and biofilm formation (biofouling).[5,6] Fine colloidal and dissolved organic compounds, including proteins, polysaccharides, and natural organic matter (NOM), are the most common foulants found in natural and wastewaters.[7−11] They can escape pretreatment and cannot be controlled by antiscalants. In addition to increasing hydraulic resistance, adsorption of dissolved organic compounds forms the conditioning layer for bacterial adhesion and subsequent biofilm development.[6,10,12] The distribution and relative abundance of the adsorbed proteins and polysaccharides has been shown to influence the biofilm structure.[13] Design of membrane materials resistant to organic fouling is a formidable challenge because our understanding of the main interactions controlling organic foulant accumulation on RO and NF membranes is limited.

The influence of membrane properties such as hydrophobicity, charge, surface roughness, and porosity on fouling has been investigated in many previous studies.[14,15] In particular, membrane surface hydrophobicity, usually determined by water contact angle measurement, was commonly related to organic fouling propensity,[4,16] although some recent studies showed that this was not always the case.[14,16] Membrane surface properties such as hydrophobicity and charge are directly determined by membrane surface chemistry.[17] Unfortunately the roles of specific chemical functionalities on membrane surfaces are largely unknown because of the physical and chemical heterogeneity resulting from the interfacial polymerization that forms the thin active barrier in RO and NF membranes.

One possible route for simplifying the problem is to study the contribution of individual chemical functionalities using well-defined and homogeneous surface chemistry. Whitesides and co-workers formed self-assembled monolayers (SAMs) of alkanethiolates with different ending chemical groups on gold surfaces to study the effect of surface wettability on nonspecific adsorption of proteins and detergents.[18] Surface wettability of each monolayer, measured by water contact angle in cyclooctane,

Received: February 18, 2011
Accepted: May 28, 2011
Revised: May 27, 2011
Published: July 06, 2011

Table 1. Characteristics of SAMs on Gold Prepared in This Study

terminal group	alkanethiol compound	contact angle[a] (deg)	thickness (nm)	XPS elemental composition (10^{-2})[b] O/C	XPS elemental composition (10^{-2})[b] N/C
$-CH_3$	1-dodecanethiol	102.6 ± 3.7	0.91	0.99	
−OPh	11-phenoxy undecanethiol	91.2 ± 3.5	0.97	8.95	
$-NH_2$	11-amino-1-undecanethiol, hydrochloride	63.3 ± 3.2	1.43	0.16	15.2
$-EG_6OH$	(1-mercapto-11-undecyl)hexa(ethylene glycol)	43.2 ± 4.3	1.62	21.4	
−COOH	11-mercaptoundecanoic acid	42.1 ± 6.7	1.25	24.6	
$-CONH_2$	11-mercaptoundecaneamide	35.7 ± 4.0	1.25	16.9	9.45
−OH	11-hydroxy-1-undecanethiol	34.2 ± 2.5	2.41	19.1	

[a] Average of 10 surfaces tested. [b] By Peak Area analysis.

was correlated to adsorption of proteins and detergents measured by surface plasmon resonance (SPR); in general, adsorption was found to be higher on low-wettability surfaces with the polyethylene glycol monolayer being an exception, to which adsorption was lower than expected. Belfort and co-workers used atomic force microscopy (AFM) to evaluate the adhesion between several proteins, including bovine serum albumin (BSA), immobilized on gold surfaces and a series of SAMs with uncharged ending functionalities formed on AFM cantilevers.[19] They found a "step-like" dependence of protein adsorption on surface wettability: surfaces with high wettability, that is, those terminated with hydroxyl, amide, and ethylene-glycol showed weak adhesion, while methyl, phenoxy, methoxy, trifluoromethyl, and nitrile (low wettability) showed high protein adhesion.

Quartz-crystal microbalance with dissipation monitoring (QCM-D) is capable of measuring minute changes in mass adsorbed on a surface.[20,21] The additional energy dissipation monitoring feature provides information on structure of the adsorbed layer. Quartz crystal sensors can be easily modified to yield a wide variety of surface chemistries. For example, gold-coated surfaces were modified by aromatic polyamide mimetic of RO membranes in our recent study.[22] In one study, adsorption of BSA on a hydrophilic (−OH) and a hydrophobic ($-CH_3$) surface was studied using a combination of quartz crystal microbalance (QCM) and grazing angle Fourier transform infrared spectroscopy.[23] It was found that BSA adsorption was accompanied by protein conformational changes and was higher on hydrophobic surfaces.[23] Other studies using similar approaches identified a number of chemical functionalities that resist protein adhesion.[24,25] In general, chemical moieties that are hydrophilic, include H-bond acceptors but do not include H-bond donors, and are electrically neutral were resistant to protein adherence.[23,25,26]

In this study we aim to elucidate the role of membrane surface chemical functionality in adsorptive fouling by common organic foulants. QCM-D was used to investigate the organic foulant adsorption equilibrium and kinetics on a variety of SAMs representing membrane surface functionalities. The effectiveness of different cleaning solutions in removing the adsorbed foulants was also evaluated. Our results suggest that membrane surface bulk properties such as hydrophobicity and charge are not reasonable predictors of organic foulant adsorption, especially for proteins. In many cases, specific interactions with individual chemical functional groups in many cases control adsorption equilibrium and kinetics as well as the removal of organic foulants by chemical cleaning. Surface modification of NF and RO membranes, therefore, should aim to minimize such specific interactions.

EXPERIMENTAL SECTION

Materials. Alkanethiols (Table 1) used to create the SAMs were purchased in either neat form or premade solutions at 1 mM in 200 proof ethanol (Asemblon, Inc., Remond, WA). Sodium alginate (10−60 kDa) derived from brown algae and BSA (∼ 66 kDa) were purchased from Sigma-Aldrich (St. Louis, MO). Surface zeta potential and hydrodynamic diameter of BSA and sodium alginate (Supporting Information (SI) Table S1) were characterized by electrophoretic mobility and dynamic light scattering (DLS) measurements using a Zetasizer Nano ZS (Malvern Instruments, Westborough, MA). Reagent grade NaCl, $CaCl_2$, NaOH, HCl and sodium-dodecyl-sulfate (SDS) were purchased from Sigma Aldrich (St. Louis, MO). All solutions were prepared using ultrapure water (≥18.1 megaΩ-cm) produced by an E-Pure system (Barnstead, Batavia, IL).

Methods. *SAM Preparation and Characterization.* Seven SAMs each with a different ending functional group (Table 1) were prepared on both gold-coated QCM-D crystals (used for adsorption experiments) and gold-coated silicon wafers (for characterization) according to our previous publication[27] with slight modifications. Silicon wafers were cleaned sequentially in acetone, methanol, and isopropanol in an ultrasonic bath (Bendeline Sonorex, London, England) followed by oxygen plasma cleaning for 5 min. They were then coated (one side polished, 330-μm thick) with a 10 nm titanium layer followed by a 30 nm gold layer at a pressure of 2×10^{-6} bar using a thermal evaporator (Odem Ltd., Rehovot, Israel).

Prior to self-assembly, gold-coated QCM-D crystals and silicon wafers were cleaned sequentially in toluene, acetone and ethanol twice in each solvent for 10 min each time in an ultrasonic bath. The substrates were then dried with ultrapure N_2 and exposed to UV/ozone in a ProCleaner chamber (Bioforce Nanosciences, Ames, IA) for 30 min. Clean substrates were first immersed in 1 mM alkanethiol solutions in ethanol for 24 h at room temperature. Prior to immersion, the pH of 11-Mercaptoundecanoic acid and 11-amino-1-undecanethiol hydrochloride solutions was adjusted to 2 and 11, respectively, using 0.2 M HCl and NH_4OH to reduce electrostatic repulsion between thiol chains and create a more ordered, homogeneous surface. After self-assembly, the substrates were transferred to 1 mM dodecanethiol solutions in ethanol for an additional 24 h, dried in ultrapure N_2 and stored under vacuum.

The chemical composition of each SAM was analyzed by X-ray photoelectron spectroscopy (XPS) using ESCALAB 250 (Thermo Fisher Scientific Inc., Waltham, UK) with an Al X-ray source and a monochromator. Since XPS analysis is destructive, measurements

were performed on SAMs formed on gold coated silicon wafers in parallel with SAMs on QCM-D crystals.

Thickness of the SAMs was estimated by Cauchy's equation[28] using an SE800 ellipsometer (Sentech Instruments GmbH, Berlin, Germany) with a light spot size of 0.5 cm^2. The phase difference between the *s* and *p* polarized waves and the amplitude attenuation were measured as a function of the wavelength from 380 to 820 nm at incidence angles of 60, 65 and 70 degrees. The optical constants of the underlying layers were determined based on measurements on a clean Au coated silicon wafer, and the refraction index of the organic layer was assumed to be 1.5,[29] which may introduce slight error in the calculated SAM thickness.

Static contact angle of water in air for the SAMs was measured using the sessile drop method with a CAM 200 contact angle analyzer (KSV Instruments LTD, Helsinki, Finland). Water drop size was approximately 2.0 μL. At least four measurements were taken per sample. Measurements were conducted immediately after preparation of the SAMs and after QCM-D adsorption and cleaning experiments. Contact angle measurements were performed using both ultrapure water and the background solutions. The results were not significantly different and only data obtained with ultrapure water are reported.

Adsorption Experiments. Adsorption of the model organic foulants was investigated using QCM-D (Q-Sense E4, Q-Sense, Glen Burnie, MD) on freshly prepared SAM coated quartz crystals. For a rigid adsorbed layer (i.e., negligible energy dissipation, ΔD), the adsorbed mass is proportional to the change in frequency as described by the Sauerbrey equation (eq 1):[30]

$$\Delta f = -\frac{2f_0^2}{A\sqrt{\rho_q \mu_q}}\Delta m \qquad (1)$$

where Δf is the change in frequency (Hz), Δm is the change in mass adsorbed (kg), f_0 is the resonant frequency (Hz) of the crystal sensor, A is the piezoelectrically active crystal area (m^2), and ρ_q and μ_q are the density (kg/m^3) and shear modulus (Pa) of quartz. For viscoelastic layers that exhibit high energy dissipations (ΔD), the vibrations amplify the shear acoustic wave such that Δf is not directly proportional to Δm. A viscoelastic model was used to fit the Δf and ΔD data simultaneously to determine the density (ρ_l), thickness (d_l), shear elastic modulus (μ_l), and viscosity (η_l) of the adsorbed layer.[31−33] All experiments were performed at 25 °C and repeated two to five times. Details of the experimental protocol are described in SI Figure S1.

RESULTS AND DISCUSSION

SAM Characterization. SAMs were characterized by XPS, ellipsometry and water drop contact angle measurements. The results are summarized in Table 1. Water contact angles measured in air were similar to data previously reported for similar SAMs[34] and the standard deviation for each sample was less than 2.0. Ellipsometry measurements showed SAMs with thickness of 0.9−2.4 nm. XPS elemental analyses support the presence of the desired functional groups. A second immersion step in dodecanethiol solution was found to improve the homogeneity of the SAM surfaces, as evident by the small standard deviation of the water contact angles. XPS and contact angle measurements made with and without the second immersion step suggest that the amount of dodecanethiol adsorbed in other SAMs was very small.

BSA and Alginate Adsorption Equilibrium on SAM Surfaces. *Adsorption Equilibrium Data Analysis.* BSA and alginate

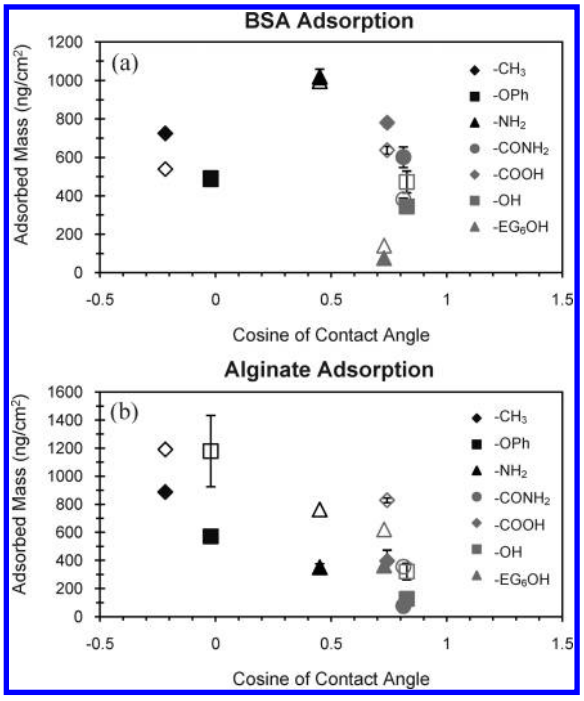

Figure 1. Calculated adsorbed mass of (a) BSA, and (b) sodium alginate on different SAMs at adsorption equilibrium. Adsorption occurred in 10 mM NaCl (solid symbols) and 7 mM NaCl/1 mM $CaCl_2$ (open symbols).

(at a concentration of 100 mg/L) were chosen as a model protein and polysaccharide, respectively, the predominant organic foulant types in wastewater.[7,10] Because Ca^{2+} has been shown to play a key role in organic fouling of NF and RO membranes,[14,35−38] adsorption experiments were performed in two electrolyte solutions: 10 mM NaCl or 7 mM NaCl and 1 mM $CaCl_2$ at an unadjusted pH of 6.0 ± 0.2.

Adsorption equilibrium occurred in all solution conditions in less than 2 h, usually within an average of 1 h. BSA adsorption in all experiments exhibited significant shift in frequency (Δf) but negligible change in dissipation (ΔD) (i.e., less than 1[21,39]), suggesting the formation of a rigid BSA layer on the SAM surface. Therefore, the Sauerbrey equation (eq 1) was applied. The calculated adsorbed mass of BSA and alginate is presented in Figure 1 as a function of water contact angle on the sensor.

Notable ΔD (greater than 1) was observed in most experiments with alginate. In a few cases when ΔD was smaller than 1 and Δf was extremely low the normalized dissipation ($\Delta D/\Delta f$) was used to determine the applicability of the Sauerbrey equation. All adsorbed alginate layers either had ΔD values greater than 1 or $\Delta D/\Delta f$ values greater than 0.1 (SI Table S2). Therefore, the visco-elastic model (Q-Tools 3.0) was used for all alginate adsorption data. Density of the alginate layer determined by fitting the raw data using the viscoelastic model ranged from 1075 to 1100 kg/m^3, consistent with previously reported values.[40] Bulk fluid density was calculated to be 997 kg/m^3, and fluid viscosity was estimated at 0.001 kg/m·s. All experiments were evaluated for the third ($n = 3$) and fifth ($n = 5$) harmonics, but only data from the third harmonic is presented.

Relationship between Organic Adsorption and Surface Wettability. Equilibrium adsorption of BSA and alginate was related to the hydrophobicity of the SAMs as measured by the cosine of water contact angle, θ (Figure 1). A correlation analysis

between $\cos(\theta)$ and adsorbed mass was performed using the Pearson product-moment coefficient (PPMC) to evaluate linear correlation and with the Spearman's rank correlation to determine monotonic dependence.[41,42] BSA adsorption in the presence and absence of calcium did not correlate with water contact angle by either analysis (Figure 1a), indicating that hydrophobicity alone is not a strong predictor of BSA adsorption.

Among the uncharged surfaces, the highly hydrophobic surfaces ($-CH_3$ and $-OPh$) adsorbed significant amounts of BSA (approximately a monolayer according to the calculated thickness), while the hydrophilic $-EG_6OH$ and $-OH$ surfaces showed low adsorption, consistent with previous studies.[19,23] The $-EG_6OH$ surface, in particular, was resistant to BSA adsorption due to its hydrophilicity and electrosteric effect.[18,26,43] Interestingly, the $-CONH_2$ surface, with a water contact angle similar to that of the $-OH$ surface, adsorbed notably higher amounts of BSA (600 ng/cm^2) in the absence of Ca^{2+}. This can be attributed to hydrogen bonding between the $-CONH_2$ surface and multiple $-NH_2$ and $-COOH$ groups on BSA. This observation is different from that by Sethuraman et al.,[19] who measured adhesion forces between four immobilized proteins and a series of chemical groups, and found similar values for $-CONH_2$, $-OH$, and $-EG_6OH$ surfaces. In their study, potential changes in molecular structure/orientation and the use of $-NH_2$ groups in immobilization of the proteins may have limited specific interactions including hydrogen bonding with the SAMs. In our study hydrogen bonding may also have contributed to BSA adsorption on the $-OH$ surface, which was higher than on $-EG_6OH$ despite a similar contact angle (Figure 1a).

The positively charged $-NH_2$ and negatively charged $-COOH$ surfaces adsorbed significantly more BSA than the $-EG_6OH$ and $-OH$ surfaces, which had similar contact angles. This is consistent with a previous study on BSA adsorption on SAMs using SPR.[44] BSA adsorption on the $-NH_2$ and $-COOH$ surfaces were similar to that on the highly hydrophobic $-CH_3$ and $-OPh$ surfaces even though the surfaces were much more hydrophilic. Adsorption on the $-NH_2$ surface was the highest likely due to the strong electrostatic attraction and acid–base interaction between the $-COO^-$ on BSA (SI Table S1, isoelectric point of BSA is 4.7–4.9[45]) and the $-NH_3^+$ on the SAM ($pK_a \sim 7.5$).[46] The high BSA adsorption on the $-COOH$ surface despite its hydrophilicity and negative charge is attributed to the charge heterogeneity of BSA: positively charged amine groups were present even though the net charge was negative. Silin et al.[44] also suggested that the presence of positively charged sites on the overall negatively charged BSA led to electrostatic interactions with the negatively charged $-COOH$ SAM.

In summary, BSA adsorption equilibrium data suggest that specific interactions, for example, between $-CONH_2$ or $-OH$ and BSA, play an important role in BSA adsorption in addition to the nonspecific electrostatic and hydrophobic interactions; charge heterogeneity can lead to significant adsorption when the overall electrostatic interaction is repulsive. Therefore, water contact angle measured in air and surface zeta potential are not good indicators for protein adsorption; membranes with higher negative zeta potential due to the presence of $-COOH$ groups may be more prone to protein fouling.

In contrast to BSA, alginate adsorption on all SAMs correlated well with water contact angle, where $-CH_3$ and $-OPh$ showed the highest adsorption (Figure 1b). Although $-EG_6OH$ surfaces have been shown to be the most resistant to protein adsorption,[18,24] alginate (polysaccharide) adsorption shows a different pattern, where the most hydrophilic surfaces ($-OH$ and $-CONH_2$) had the lowest adsorption (Figure 1b). The mass of alginate adsorbed on the hydrophilic surfaces was less than that of a monolayer, indicating patched adsorption (Figure S2). Although alginate has been reported to foul NF and RO membranes more severely than BSA,[47,48] our measurements show similar adsorption of both onto clean surfaces, indicating the greater fouling rate of alginate is likely due to faster gel layer formation due to increased foulant–foulant interactions.

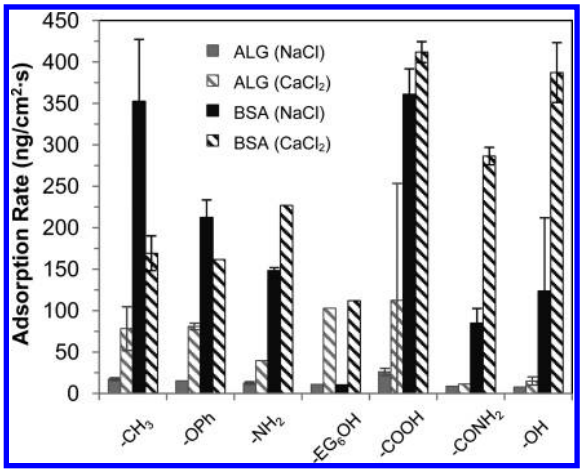

Figure 2. Initial adsorption rate of BSA and alginate.

Effect of Calcium on Adsorption. Calcium showed an intense effect on alginate adsorption and moderate effect on BSA adsorption. The effect of Ca^{2+} on BSA adsorption depended on the particular surface functionality. In the presence of Ca^{2+}, BSA adsorption on the $-CONH_2$ and $-COOH$ surfaces decreased (Figure 1a). This is attributed to complexation of Ca^{2+} with $-COO^-$ on both BSA and the SAM, reducing the number of $-COO^-$ sites available for adsorption. BSA adsorption increased on the $-OH$ surface and decreased on $-CH_3$. This could be explained by changes in surface interaction energy of BSA and the SAMs, as has been shown for alginate and RO membranes.[49]

Addition of Ca^{2+} increased alginate adsorption intensely on all SAMs tested (Figure 1b). Alginate has the propensity to aggregate and form cation-stabilized gels due to a high carboxyl content (approximately 61% mannuronic acid and 39% guluronic acid).[49,50] Ca^{2+} has also been reported to decrease the cohesive free energy of alginate and the free energy of adhesion between alginate and RO membranes.[49] As a result, both the adsorbed mass (Figure 1b) and adsorbed layer thickness (Figure S2) of alginate increased in the presence of Ca^{2+}. The gel formation was also evident in the increased viscosity of all adsorbed alginate layers (Figure S2).

Surface Chemistry Effect on Adsorption Kinetics. Adsorption kinetics of organic foulants is important as it is related to the initial fouling rate on a clean membrane as well as changes in membrane surface properties. Mass adsorption kinetics curves of BSA and alginate were obtained from time-resolved Δf and ΔD data, and the initial adsorption rate determined from the linear section of the kinetics curve was shown in Figure 2.

Despite comparable adsorbed mass at equilibrium (Figure 1), initial fouling rates on all SAMs were markedly higher for BSA than alginate (Figure 2). This result suggests that proteins could be a dominant component in the initial conditioning layer and

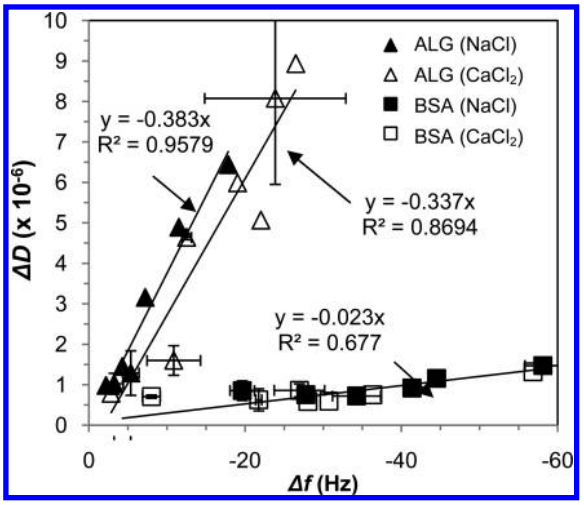

Figure 3. Measured dissipation change (ΔD) and frequency change (Δf) at adsorption equilibrium.

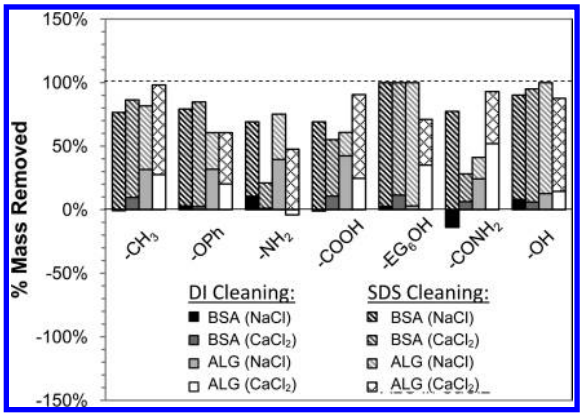

Figure 4. Stacked bar graph indicating % mass of adsorbed layer removed by DI (solid) and 2% SDS cleaning (pattern).

consequently play a critical role in membrane biofouling even though its quantity in the fouling layer may be low. Adsorption kinetics of both BSA and alginate strongly depended on the type of SAM. In NaCl, BSA initial adsorption rate followed the order of $-COOH > -CH_3 > -OPh > -NH_2 > -OH > -CONH_2 > -EG_6OH$, showing no correlation to water contact angle. The presence of Ca^{2+} increased BSA adsorption rate on most SAMs except for the two most hydrophobic surfaces, $-CH_3$ and $-OPh$, on which BSA adsorption decreased compared to that in NaCl.

Initial alginate adsorption rates were much lower than those of BSA (Figure 2) and were consistently higher in the presence of Ca^{2+} on all SAMs, even though alginate formed large aggregates in solution (SI Table S1), which reduces the diffusive mass transfer rate. This increase in adsorption rate is attributed to enhanced alginate-alginate attraction and is consistent with increased membrane fouling rates observed with alginate in the presence of Ca^{2+}.[51]

The $-COOH$ surface showed the greatest initial adsorption rate for both BSA and alginate. These results suggest higher initial protein and polysaccharide fouling rates on membranes that expose $-COOH$ groups and further support that specific interactions may delineate fouling properties more accurately than nonspecific hydrophobic interactions.

Adsorbed Layer Structure. In addition to the total mass and thickness, the structure of the organic gel layer plays a critical role in determining the hydraulic resistance of the gel layer. The normalized dissipation, $\Delta D/\Delta f$, provides structural information of the adsorbed layer. Figure 3 presents ΔD as a function of Δf at adsorption equilibrium for both BSA and alginate. The BSA or alginate layers formed on different SAMs showed similar normalized dissipation, indicating that surface chemistry did not affect the structure of the adsorbed layer at equilibrium. All alginate layers exhibited much higher $\Delta D/\Delta f$ than the BSA layers, showing that alginate layers are looser and more elastic than the BSA layers. The rigid structure of the BSA layer was not affected by Ca^{2+}, while the alginate layer in the presence of Ca^{2+} is denser and probably more cross-linked. However, this effect cannot be observed in Figure 3 because the increase in $\Delta D/\Delta f$ due to higher viscosity counter balances the effect of higher density. A similar plot of ΔD vs Δf during the adsorption process illustrates the dynamic change of the adsorbed layer structure (SI Figure S3). BSA adsorption exhibited a two−phase growth with notable faster increase in ΔD in the second phase, suggesting changes in BSA molecular conformation or orientation.[23,44,52] Such change in structure strongly depended on the SAM ending functionality.

These results suggest that membrane surface chemistry may not affect the specific resistance of BSA or alginate fouling layer at adsorption equilibrium. However, when other foulants are also present, which is the case for any natural water or wastewater, the impact of surface chemistry on the initial structure of the adsorbed protein layer may play a role in the subsequent attachment of other foulants (e.g., mineral precipitates and bacterial cells) and consequently the structure of the fouling layer.

Cleaning of Adsorbed Organic Foulants on SAMs. The responses of the adsorbed foulants to pure water and surfactant cleaning with 2% SDS were evaluated sequentially based on the fraction of mass removed (Figure 4). DI water rinsing was not very effective, with −14 to 52% removal (negative values resulted from adsorbed layer swelling). SDS cleaning was more effective, removing 21−100% of the adsorbed mass. In general, cleaning efficiency for alginate was much greater than for BSA, indicating that proteins may contribute to irreversible fouling more than polysaccharides. Although the two most hydrophobic SAMs ($-CH_3$ and $-OPh$) adsorbed a large amount of BSA and alginate, the adsorbed foulants can be removed relatively effectively by SDS cleaning. SAMs of $-NH_2$, $-COOH$, and $-CONH_2$, however, consistently showed significant residual BSA and/or alginate. Despite the importance of Ca^{2+} in adsorption equilibrium and kinetics, Ca^{2+} did not significantly affect BSA irreversible fouling of any SAMs except the $-NH_2$ and $-CONH_2$ surface, for which irreversible fouling increased greatly in the presence of Ca^{2+}. This phenomena was extended to $-NH_2$ for alginate. These results indicate that $-CONH_2$ and especially $-NH_2$ on membrane surfaces may contribute more to irreversible fouling of NF and RO membranes than other functional groups under typical wastewater solution conditions due to increased hydrogen bonding.

Implications for Membrane Fouling. Understanding factors controlling organic foulant adsorption on NF and RO membranes is important for developing fouling resistant membranes and other fouling control strategies such as pretreatment and chemical cleaning. Our study shows evidence for the first time

that specific interactions, such as hydrogen bonding and electrostatic interactions between specific functionalities, play a more important role than nonspecific electrostatic and hydrophobic interactions in adsorption of and irreversible fouling by proteins and polysaccharides. Because the initial adsorption of proteins and polysaccharides (i.e., surface conditioning) has important impacts on the subsequent formation of scales and biofilms, these results suggest that specific surface functionality may be more important than bulk surface properties, such as zeta potential and hydrophobicity, in long-term fouling and cleaning of NF and RO membranes. Therefore, surface modifications of NF and RO membranes that minimize functionalities causing hydrogen bonding as well as charged sites (e.g., $-COOH$, $-NH_2$) may be an effective approach to develop fouling resistant membranes. We also show for the first time that proteins, although usually found in smaller quantity on fouled membranes,[53,54] adsorb much faster to functional groups typically found on NF and RO membrane surfaces and are more difficult to remove by chemical cleaning than polysaccharides. These results suggest that proteins play an important role in initiating biofouling despite their smaller quantity. Therefore, pretreatment and chemical cleaning methods should also target protein removal.

■ ASSOCIATED CONTENT

Supporting Information. Details of the QCM-D protocol, raw data, and layer structure. This material is available free of charge via the Internet at http://pubs.acs.org.

■ AUTHOR INFORMATION

Corresponding Author
*E-mail: Qilin.li@rice.edu (Q.L.); kasher@bgu.ac.il (R.K.).

■ ACKNOWLEDGMENT

Financial support was awarded through an NSF grant (Q.L., No. CBET-0552413a) and the German-Israeli BMBF-MOST Water Research Program (R.K., grant WT0902). Graduate and postdoctoral support was provided by the Department of Homeland Security and the Blaustein Center for Scientific Cooperation, Ben-Gurion University of the Negev, respectively. Special thanks to Bo Chen, Costa Abarbanel, Natalya Froumin, and Jürgen Jopp for their assistance.

■ REFERENCES

(1) Petersen, R. J. Composite reverse osmosis and nanofiltration membranes. *J. Membr. Sci.* **1993**, *83*(1), 81−150, DOI: 10.1016/0376-7388(93)80014-O.

(2) Kilduff, J. E.; Mattaraj, S.; Zhou, M.; Belfort, G. Kinetics of membrane flux decline: The role of natural colloids and mitigation via membrane surface modification. *J. Nanopart. Res.* **2005**, *7*(4), 525−544, DOI: 10.1007/s11051-005-5043-y.

(3) Li, Q. L.; Elimelech, M. Organic fouling and chemical cleaning of nanofiltration membranes: Measurements and mechanisms. *Environ. Sci. Technol.* **2004**, *38*(17), 4683−4693. DOI: 10.1021/es0354162.

(4) Violleau, D.; Essis-Tome, H.; Habarou, H.; Croué, J. P.; Pontié, M. Fouling studies of a polyamide nanofiltration membrane by selected natural organic matter: An analytical approach. *Desalination* **2005**, *173*(3), 223−238. DOI: 10.1016/j.desal.2004.07.048.

(5) Flemming, H. C.; Schaule, G.; Griebe, T.; Schmitt, J.; Tamachkiarowa, A. Biofouling—The achilles heel of membrane processes. *Desalination* **1997**, *113*(2−3), 215−225. DOI: 10.1016/S0011-9164(97)00132-X.

(6) Baker, J. S.; Dudley, L.Y.Biofouling in membrane systems—A review. *Desalination* **1998**, *118*(1−3), 81−89, DOI: 10.1016/S0011-9164(98)00091-5.

(7) Jarusutthirak, C.; Amy, G.; Croué, J.-P.Fouling characteristics of wastewater effluent organic matter (EfOM) isolates on NF and UF membranes. *Desalination* **2002**, *145*(1−3), 247−255. DOI:10.1016/S0011-9164(02)00419-8.

(8) Cho, J.; Amy, G.; Pellegrino, J.; Yoon, Y. Characterization of clean and natural organic matter (NOM) fouled NF and UF membranes, and foulants characterization. *Desalination* **1998**, *118*(1−3), 101−108. DOI: 10.1016/S0011-9164(98)00100-3.

(9) Cho, J.; Amy, G.; Pellegrino, J.Membrane filtration of natural organic matter: Initial comparison of rejection and flux decline characteristics with ultrafiltration and nanofiltration membranes. *Water Res.* **1999**, *33*(11), 2517−2526, DOI: 10.1016/S0043-1354(98)00498-9.

(10) Jarusutthirak, C.; Amy, G. Understanding soluble microbial products (SMP) as a component of effluent organic matter (EfOM). *Water Res.* **2007**, *41*(12), 2787−2793, DOI: 10.1016/j.watres.2007.03.005.

(11) Rebhun, M.; Manka, J.Classification of organics in secondary effluents. *Environ. Sci. Technol.* **1971**, *5*(7), 606−609, DOI: 10.1021/es60054a004.

(12) Howe, K. J.; Clark, M. M.Fouling of microfiltration and ultrafiltration membranes by natural waters. *Environ. Sci. Technol.* **2002**, *36*(16), 3571−3576, DOI: 10.1021/es025587r.

(13) Chen, M.-Y.; Lee, D.-J.; Yang, Z.; Peng, X. F.; Lai, J.Y. Fluorecent staining for study of extracellular polymeric substances in membrane biofouling layers. *Environ. Sci. Technol.* **2006**, *40*(21) 6642−6646, DOI: 10.1021/es0612955.

(14) Combe, C.; Molis, E.; Lucas, P.; Riley, R.; Clark, M.M. The effect of ca membrane properties on adsorptive fouling by humic acid. *J. Membr. Sci.* **1999**, *154*(1), 73−87, DOI: 10.1016/S0376-7388(98)-00268-3.

(15) Kilduff, J. E.; Mattaraj, S.; Pieracci, J.P.; Belfort, G. Photochemical modification of poly(ether sulfone) and sulfonated poly(sulfone) nanofiltration membranes for control of fouling by natural organic matter. *Desalination* **2000**, *132*(1−3), 133−142, DOI: 10.1016/S0011-9164(00)00142-9.

(16) Li, Q.; Xu, Z.; Pinnau, I. Fouling of reverse osmosis membranes by biopolymers in wastewater secondary effluent: Role of membrane surface properties and initial permeate flux. *J. Membr. Sci.* **2007**, *290*(1−2), 173−181, DOI: 10.1016/j.memsci.2006.12.027.

(17) Morgan, P. W.; Kwolek, S. L. Interfacial polycondensation. II. Fundamentals of polymer formation at liquid interfaces. *J. Polym. Sci., Part A-1: Polym. Chem.* **1996**, *34* (4), 531–559.

(18) Sigal, G. B.; Mrksich, M.; Whitesides, G.M. Effect of surface wettability on the adsorption of proteins and detergents. *J. Am. Chem. Soc.* **1998**, *120*(14), 3464−3473, DOI: 10.1021/ja970819l.

(19) Sethuraman, A.; Han, M.; Kane, R.S.; Belfort, G. Effect of surface wettability on the adhesion of proteins. *Langmuir* **2004**, *20*(18), 7779−7788, DOI: 10.1021/la049454q.

(20) Höök, F. *Development of a Noval QCM Technique for Protein Adsorption Studies*; Department of Biochemistry and Biophysics and Department of Applied Physics. Chalmers University of Technology, Götebory University: Göteborg, Sweden, 1997; p 60.

(21) Höök, F.; Rodahl, M.; Brzezinski, P.; Kasemo, B. Energy dissipation kinetics for protein and antibody-antigen adsorption under shear oscillation on a quartz crystal microbalance. *Langmuir* **1998**, *14*(4), 729−734, DOI: 10.1021/la970815u.

(22) Steiner, Z.; Miao, J.; Kasher, R. Development of an oligoamide coating as a surface mimetic for aromatic polyamide films used in reverse osmosis membranes. *Chem. Commun.* **2011**, *47*(8), 2384−2386, DOI: 10.1039/C0CC04379F.

(23) Roach, P.; Farrar, D.; Perry, C. C. Interpretation of protein adsorption: Surface-induced conformational changes. *J. Am. Chem. Soc.* **2005**, *127*(22), 8168−8173, DOI: 10.1021/ja042898o.

(24) Ostuni, E.; Chapman, R. G.; Holmlin, R. E.; Takayama, S.; Whitesides, G. M. A survey of structureâ'property relationships of surfaces that resist the adsorption of protein. *Langmuir* **2001**, *17* (18), 5605–5620.

(25) Chapman, R. G.; Ostuni, E.; Liang, M. N.; Meluleni, G.; Kim, E.; Yan, L.; Pier, G.; Warren, H. S. ; Whitesides, G.M. Polymeric thin films that resist the adsorption of proteins and the adhesion of bacteria. *Langmuir* **2001**, *17*(4), 1225−1233, DOI: 10.1021/la001222d.

(26) Ostuni, E.; Chapman, R.G.; Holmlin, R. E.; Takayama, S.; Whitesides, G. M. A survey of structure-property relationships of surfaces that resist the adsorption of protein. *Langmuir* **2001**, *17*(18), 5605−5620, DOI: 10.1021/la010384m.

(27) Steiner, Z.; Rapaport, H.; Oren, Y.; Kasher, R. Effect of surface-exposed chemical groups on calcium-phosphate mineralization in water-treatment systems. *Environ. Sci. Technol.* **2010**, *44*(20), 7937−7943. DOI: 10.1021/es101773t.

(28) Jenkins, F. A.; White, H. E. *Fundamentals of Optics*, 4th ed.; McGraw-Hill Inc.: New York, 1981.

(29) Brunner, H.; Vallant, T.; Mayer, U.; Hoffmann, H. Formation of ultrathin films at the solid-liquid interface studied by in situ ellipsometry. *J. Colloid Interface Sci.* **1999**, *212*(2), 545−552, DOI: 10.1006/jcis.1998.6062.

(30) Sauerbrey, G. Verwendung von schwingquarzen zur wagung diinner schicten und zur mikrowagung. *Z. Phys.* **1959**, *155*(1), 206−222, DOI: 10.1007/BF01337937.

(31) Bandey, H. L.; Hillman, A.R.; Brown, M. J.; Martin, S.J. Viscoelastic characterization of electroactive polymer films at the electrode/solution interface. *Faraday Discuss.* **1997**, *107*(1), 105−121, DOI: 10.1039/A704278G.

(32) Voinova, M. V. et al. Viscoelastic acoustic response of layered polymer films at fluid-solid interfaces: Continuum mechanics approach. *Phys. Scr.* **1999**, *59*(5), 391, DOI: 10.1238/Physica.Regular.059a00391.

(33) Diethelm, J. Viscoelastic analysis of organic thin films on quartz resonators. *Macromol. Chem. Phys.* **1999**, *200*(3), 501−516, DOI: 10.1002/(SICI)1521-3935(19990301)200:3<501::AID-MACP501>3.0.CO;2-W.

(34) Tanahashi, M.; Matsuda, T. Surface functional group dependence on apatite formation on self-assembled monolayers in a simulated body fluid. *J. Biomed. Mater. Res.* **1997**, *34*(3), 305−315, DOI: 10.1002/(SICI)1097-4636(19970305)34:3<305::AID-JBM5>3.3.CO;2-4.

(35) Rice, G.; Barber, A.; A. O'Connor; Stevens, G.; Kentish, S. Fouling of NF membranes by dairy ultrafiltration permeates. *J. Membr. Sci.* **2009**, *330*(1−2), 117−126, DOI: 10.1016/j.memsci.2008.12.048.

(36) Mo, H.; Tay, K.G.; Ng, H. Y. Fouling of reverse osmosis membrane by protein (bsa): Effects of ph, calcium, magnesium, ionic strength and temperature. *J. Membr. Sci.* **2008**, *315*(1−2), 28−35, DOI:10.1016/j.memsci.2008.02.002.

(37) Broeckmann, A.; Wintgens, T.; A. I. Schäfer Removal and fouling mechanisms in nanofiltration of polysaccharide solutions. *Desalination* **2005**, *178*(1−3), 149−159, DOI: 10.1016/j.desal.2004.12.017.

(38) Seidel, A.; Elimelech, M. Coupling between chemical and physical interactions in natural organic matter (NOM) fouling of nanofiltration membranes: Implications for fouling control. *J. Membr. Sci.* **2002**, *203*(1−2), 245−255, DOI:10.1016/S0376-7388(02)00013-3.

(39) Hook, F.; Kasemo, B.; Nylander, T.; Fant, C.; Sott, K.; Elwing, H. Variations in coupled water, viscoelastic properties, and film thickness of a Mefp-1 protein film during adsorption and cross-linking: A quartz crystal microbalance with dissipation monitoring, ellipsometry, and surface plasmon resonance study. *Anal. Chem.* **2001**, *73*(24), 5796−5804, DOI: 10.1021/ac0106501.

(40) Scott, E. A.; Nichols, M. D.; Cordova, L. H.; George, B. J.; Jun, Y.-S.; Elbert, D. L. Protein adsorption and cell adhesion on nanoscale bioactive coatings formed from poly(ethylene glycol) and albumin microgels. *Biomaterials* **2008**, *29* (34), 4481–4493.

(41) Rodgers, J. L.; Nicewander, W. A. Thirteen ways to look at the correlation coefficient. *Am Stat.* **1988**, *42* (1), 59–66.

(42) Myers, J. L.; Well, A.D. *Research Design and Statistical Analysis*, 2nd ed.; Lawrence Erlbaum Associate: Hillsdale, NJ, 2003.

(43) Herrwerth, S.; Eck, W.; Reinhardt, S.; Grunze, M. Factors that determine the protein resistance of oligoether self-assembled monolayers—Internal hydrophilicity, terminal hydrophilicity, and lateral packing density. *J. Am. Chem. Soc.* **2003**, *125*(31), 9359−9366, DOI: 10.1021/ja034820y.

(44) Silin, V.; Weetall, H.; Vanderah, D.J. Spr studies of the non-specific adsorption kinetics of human IgG and BSA on gold surfaces modified by self-assembled monolayers (SAMs). *J. Colloid Interface Sci.* **1997**, *185*(1), 94−103, DOI: 10.1006/jcis.1996.4586.

(45) Nakamura, K.; Matsumoto, K. Properties of protein adsorption onto pore surface during microfiltration: Effects of solution environment and membrane hydrophobicity. *J. Membr. Sci.* **2006**, *280* (1−2), 363–374.

(46) Degefa, T. H.; P. Schön; Bongard, D.; Walder, L. Elucidation of the electron transfer mechanism of marker ions at sams with charged head groups. *J. Electroanal. Chem.* **2004**, *574*(1), 49−62, DOI: 10.1016/j.jelechem.2004.07.026.

(47) Kim, S.; Hoek, E.M.V. Interactions controlling biopolymer fouling of reverse osmosis membranes. *Desalination* **2007**, *202*(1−3), 333−342, DOI: 10.1016/j.desal.2005.12.072.

(48) Contreras, A. E.; Kim, A.; Li, Q. Combined fouling of nanofiltration membranes: Mechanisms and effect of organic matter. *J. Membr. Sci.* **2009**, *327*(1−2), 87−95, DOI: 10.1016/j.memsci.2008.11.030.

(49) Jin, X.; Huang, X.; Hoek, E. M. V. Role of specific ion interactions in seawater ro membrane fouling by alginic acid. *Environ. Sci. Technol.* **2009**, *43*(10), 3580−3587, DOI: 10.1021/es8036498.

(50) Chen, K. L.; Elimelech, M. Influence of humic acid on the aggregation kinetics of fullerene (c60) nanoparticles in monovalent and divalent electrolyte solutions. *J. Colloid Interface Sci.* **2007**, *309*(1), 126−134. DOI: 10.1016/j.jcis.2007.01.074.

(51) Hashino, M.; Katagiri, T.; Kubota, N.; Ohmukai, Y.; Maruyama, T.; Matsuyama, H. Effect of membrane surface morphology on membrane fouling with sodium alginate. *J. Membr. Sci.* **2010**, *366*(1−2), 258−265, DOI: 10.1016/j.memsci.2010.10.014.

(52) Nakata, S.; Kido, N.; Hayashi, M.; Hara, M.; Sasabe, H.; Sugawara, T.; Matsuda, T. Chemisorption of proteins and their thiol derivatives onto gold surfaces: Characterization based on electrochemical nonlinearity. *Biophysical Chemistry* **1996**, *62*(1−3), 63−72, DOI: 10.1016/S0301-4622(96)02208-9.

(53) Le-Clech, P.; Chen, V.; Fane, T. A. G. Fouling in membrane bioreactors used in wastewater treatment. *J. Membr. Sci.* **2006**, *284*(1−2), 17−53, DOI: 10.1016/j.memsci.2006.08.019.

(54) Park, N.; Lee, S.; Yoon, S.R.; Kim, Y.H.; Cho, J. Foulants analyses for nf membranes with different feed waters: Coagulation/sedimentation and sand filtration treated waters. *Desalination* **2007**, *202*(1−3), 231−238, DOI: 10.1016/j.desal.2005.12.060.